Applied Energy 365 (2024) 123151

Contents lists available at ScienceDirect

Applied Energy

journal homepage: www.elsevier.com/locate/apenergy

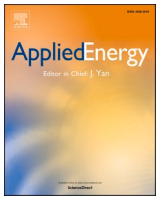

System-cost-minimizing deployment of PV-wind hybrids in low-carbon U.S. power systems

Patrick R. Brown *, Travis Williams, Maxwell L. Brown, Caitlin Murphy

National Renewable Energy Laboratory, Golden, CO, USA

HIGHLIGHTS

- PV-wind hybrid deployment is modeled at ~50,000 sites across the contiguous U.S.
- Hundreds of gigawatts of PV-wind hybrids are deployed in modeled zero-carbon systems.
- With hybridization, PV capacity often relocates to sites with installed wind capacity.
- Overall electricity system costs are reduced by roughly 1–2% with hybridization.
- "Overbuilding" generation vs interconnection capacity offsets high transmission costs.

ARTICLE INFO

Keywords:
Hybrid renewable energy systems
Wind
Solar
Capacity expansion modeling
Decarbonization

ABSTRACT

Hybridization of solar photovoltaic (PV) and wind installations has the potential to reduce transmission costs through sharing of spur-line capacity and other interconnection cost components. Many studies have assessed hybridization opportunities on a site-by-site basis but have not captured the impact of PV-wind hybridization on overall power system evolution and system costs. Here, we use a high-resolution national-scale capacity-expansion model to explore electricity-system-cost-minimizing deployment of PV-wind hybrid systems across the United States (U.S.) in scenarios that achieve a zero-carbon electricity mix in 2040. While overall system cost savings resulting from hybridization are relatively small—roughly 0.8% for baseline interconnection cost assumptions and <2% for sensitivity cases with high interconnection costs—there are notable shifts in deployment patterns when hybridization is allowed. PV capacity is often relocated to sites where wind capacity and associated interconnection capacity is already deployed, and "overbuilding" of nameplate PV and wind capacity relative to point-of-interconnection capacity is observed to increase with rising interconnection costs. Roughly 300 gigawatts (GW) of point-of-interconnection capacity (over 500 GW of nameplate PV and wind capacity) are deployed at hybrid installations with PV:wind capacity ratios between 1:3 and 3:1 in modeled zero-carbon power systems across the U.S.

1. Introduction

The deployment of large-scale solar photovoltaic (PV) and land-based wind generation capacity has grown in recent years due to a combination of technology advancement and policy drivers. Such trends are expected to continue going forward, as many studies show that rapid near-term deployment of PV and wind generation capacity is the lowest-cost approach for meeting electricity-sector decarbonization goals [1–3].

As PV and wind deployment rates increase, the logistics and costs of grid interconnection – including power-flow studies incorporating the impacts of new generators, permitting and construction of new "spur lines" connecting PV and wind to nearby transmission features, and reinforcement of the existing transmission network to support increased power flows – have emerged as a bottleneck limiting accelerated expansion [4–6]. These challenges motivate interest in the colocation and/or "hybridization" of PV and wind generation technologies; in such configurations, PV and wind generation capacity share the same point of interconnection (POI) to the transmission network, and they may also share power electronics and controls [7].

Many drivers contribute to interest in hybrid PV + wind (HPW) plants in the United States, including avoided transmission upgrades,

* Corresponding author.
E-mail address: Patrick.Brown@nrel.gov (P.R. Brown).

https://doi.org/10.1016/j.apenergy.2024.123151
Received 10 December 2023; Received in revised form 29 February 2024; Accepted 31 March 2024
Available online 20 April 2024
0306-2619/© 2024 The Authors. Published by Elsevier Ltd. This is an open access article under the CC BY license (http://creativecommons.org/licenses/by/4.0/).

reduced development and financing costs, and flatter plant-level power output [8–10]. Industry interest is apparent in the form of both existing projects and interconnection queues across the United States; as of the end of 2021, there were nine operating HPW projects in the United States, comprising over 1 gigawatt (GW) of PV and wind generation capacity. An additional 27 projects—totaling 10 GW of additional generation capacity—have been proposed in U.S. interconnection queues, some of which further include an energy storage component to enhance operational flexibility. On average, the wind component makes up a larger share of the generation capacity in both existing and proposed HPW projects in the United States, and HPW projects represent almost half of proposed wind-based hybrid capacity in those queues [11].

In situations where the cost of new variable generation capacity ($/kW$_{gen}$) is low relative to the cost of interconnection ($/kW$_{POI}$), some amount of "overbuilding" of generation capacity relative to POI capacity (such that kW$_{gen}$ > kW$_{POI}$; for example, procuring 100 MW of POI capacity for a 130 MW nameplate PV array) is likely to be cost-optimal even for a single resource type. If a PV array only reaches its peak output for a few hours of the year, it is more economic to size the POI for more typical generation conditions and increase the average utilization of the POI, even if some energy is curtailed (or "clipped") during times of peak generation. Overbuilding a combination of PV and wind at a single site (kW$_{PV}$ + kW$_{wind}$ > kW$_{POI}$) can lead to higher POI utilization and lower cost than overbuilding a single resource type, particularly in locations where the temporal availability of PV and wind resources is uncorrelated or anticorrelated.

In the U.S. context, the ability to overbuild generation capacity relative to interconnection capacity (or, equivalently, to underbuild interconnection capacity) is codified in federal and regional rules [12]. At the federal level, FERC Order 845 allows a generator to request interconnection service below the generation facility's capacity rating while recognizing the need to ensure that the generation facility does not inject energy above the requested level of service. At the scale of a regional transmission operator (RTO) or independent system operator (ISO), similar programs are already in place in the California (CAISO), Midwest (MISO), New England (ISONE), and Pennsylvania-New Jersey-Maryland (PJM) ISOs, typically with a requirement for additional monitoring or control technologies to enforce (or allow the ISO to enforce) the approved interconnection service level.

Many previous studies have explored the design and potential of utility-scale HPW systems from a variety of perspectives [13], including temporal complementarity, configurations, control, and sizing [14–18]. The temporal complementarity of PV and wind production has been extensively explored at multiple spatial scales—ranging from global [19] to regional—through the evaluation of statistical correlation metrics and indices [20]. Such studies identify locations with characteristics that may be indicative of hybridization benefits, but they are rooted exclusively in resource potential and production and thus do not account for economic competitiveness.

The economic potential of HPW has been estimated based on levelized cost of energy (LCOE) [21,22] or plant-level profitability from the perspective of the plant owner [23–25]. While such approaches offer useful insights, they are limited in their ability to inform economic deployment potential. In particular, LCOE is an incomplete metric for evaluating the competitiveness of system resources because it does not account for the value that such a resource could provide to the electricity system. In addition, plant-level profitability may not translate into net economic value for the system as a whole. To our knowledge, no studies have explored HPW system designs that minimize the total system cost of electricity at the scale of the United States in a fully featured capacity-expansion model (CEM).

Here, we demonstrate HPW deployment in a CEM with high spatial resolution (~50,000 sites across the contiguous U.S., modeled as 11 independent regions) and moderate temporal resolution (780 2-h timeslices), focusing on a scenario that reaches zero electricity-sector carbon emissions by 2040. HPW system designs are independently optimized at each potential installation site, identifying the PV nameplate, wind nameplate, and shared POI (spur line plus network reinforcement) capacities that minimize overall electricity system cost. We show that spatial trends in system-cost-minimizing HPW deployment differ from the results of a site-by-site LCOE-minimizing model. Hundreds of gigawatts (GW) of HPW capacity are deployed in a cost-optimal zero-carbon system, but the overall electricity system cost savings from hybridization are <1% under central cost assumptions. Allowing interconnection cost sharing via hybridization changes spatial patterns of PV and wind deployment but does not have a large impact on the total amount of PV and wind capacity deployed within the set of geographic, technical, and policy assumptions analyzed here.

2. Methods

2.1. Capacity-expansion model

For this study, we use a version of the Regional Energy Deployment System (ReEDS) CEM developed at the U.S. National Renewable Energy Laboratory (NREL). ReEDS optimizes the capacity and operation of bulk generation, transmission, and storage assets to minimize total system cost—subject to a range of constraints on resource availability, plant characteristics, energy balance, resource adequacy, and state and federal policies—in 1–5 year sequential timesteps. The ReEDS model is described in detail by Ho et al. [26] and a number of other studies [27]. Here we describe only the additions and modifications made to the default temporal resolution, spatial resolution, and interconnection representation in ReEDS (v2022) to enable an adequate representation of HPW generators.

2.1.1. Temporal resolution

Previous versions of the ReEDS model used a combination of time resolutions. Transmission flows and the seasonal availability of renewable energy were represented by 17 timeslices (4 per season, plus a peak timeslice representing the 40 highest-demand hours in summer). Between each sequential solve year, additional calculations of marginal and existing variable renewable energy (VRE) curtailment, storage energy arbitrage value, and capacity credit for VRE and storage were calculated using hourly load and VRE availability over one or more full years (1 year × 8760 h for curtailment and arbitrage; 7 years × 8760 h for capacity credit), with the resulting marginal parameters used in the next sequentially modeled year [28].

17 timeslices are insufficient to accurately capture the temporal complementarity of wind and solar availability and the clipping that results from oversizing PV and wind generators relative to POI capacity (both of which are necessary to accurately represent HPW operation). Here we instead model 10 representative 5-day periods and 3 outlying 5-day periods (65 days total) from weather year 2012 with 2-h resolution. Representative periods are identified by hierarchical clustering, with regional load, solar, and wind profiles used as features with a weighting of 1:0.5:0.5 (respectively). The three outlier 5-day periods comprise the period with minimum average solar availability; the period with minimum average wind availability; and the period containing the peak load hour. The inter-year calculations of marginal curtailment and storage arbitrage value that accompany the 17-timeslice version of ReEDS are discarded, but the 7 × 8760 calculation of capacity credit is retained. Additional details regarding representative-period selection and increased time resolution in ReEDS are discussed by Brown et al. [29].

2.1.2. Spatial resolution

ReEDS includes ~1900 unique hourly availability profiles for utility-scale PV and onshore wind resources. These profiles are spread across the intersection of 134 model zones with 7 resource classes (defined by annual average irradiance) for PV and the intersection of 356 resource regions with 10 resource classes (defined by annual average wind speed) for onshore wind. The available land area for PV and wind deployment is

quantified by the separate Renewable Energy Potential (reV) model at >56,000 grid cells of ~11.5 km × 11.5 km area [30]. For each grid cell, the cost of a transmission "spur line" connecting the center of the cell to an interconnection feature on the existing transmission system (a substation, a tie-in point on a transmission line, or the edge of an urban load center) is estimated, combining terrain-specific cost modifiers with regionally varying $/MW-mile base costs. Previous ReEDS versions included different estimates for spur-line costs between PV and wind at a given grid cell, including the effects of economies of scale; here we use a technology-agnostic estimate based on a uniform 400 MW plant size. Fig. 1a shows the spur-line costs at the >56,000 grid cells used in this study, calculated using the methods and data described by Lopez et al. [31].

Typically, the grid cells associated with a given resource region and resource class are aggregated into "bins" (5 bins per region/class for wind and 20 bins per region/class for PV) to decrease problem size, reducing the combined number of unique PV and wind investment options from >110,000 (>56,000 each for PV and wind) to ~11,000. Here, to capture the site-specific nature of spur-line sharing for HPW, we do not aggregate grid cells, instead tracking PV capacity, wind capacity, and spur-line cost and capacity for each of the >56,000 sites. Hourly availability profiles for PV and wind are kept at their original resolution; a single hourly availability profile is shared across all sites in the same region/class combination.

In sum, the temporal resolution is increased by >40× and the spatial resolution of PV/wind capacity deployment is increased by ~10× in this study compared to previous applications of the ReEDS model. The ReEDS model is typically used to model the entire contiguous US in a single optimization framework, but doing so at the increased temporal and spatial resolution used here leads to intolerable computation times. We therefore run independent optimizations over the 11 smaller "transmission regions" shown in Fig. 1b, modeled after the transmission planning regions in FERC Order 1000 [32] plus the Electric Reliability Council of Texas (ERCOT). As such, we do not capture the value of transmission between these regions, which previous studies have identified as an important cost-saving opportunity in decarbonized electricity systems [33].

2.1.3. Interconnection sharing

In previous applications of the ReEDS model, the site-specific interconnection cost was combined with the site-specific PV or wind cost, and a 1 MW_{AC} investment in PV or wind was always implicitly accompanied by a 1 MW_{AC} investment in POI capacity (comprising a spur line and associated bulk network reinforcement). Here, we instead introduce new variables and constraints allowing POI capacity and PV/wind capacity to be independently optimized, accounting for "clipping" when hourly generation from PV and wind at a given site is greater than the POI capacity. The combined availability of energy from a hybrid site x is limited by the PV and wind capacity and capacity factor:

$$A_{x,h,t} \leq C_{\mathrm{PV},x,t} \bullet \lambda_{\mathrm{PV},x,h,t} + C_{\mathrm{wind},x,t} \bullet \lambda_{\mathrm{wind},x,h,t} \forall (x,h,t) \quad (1)$$

and by the POI capacity:

$$A_{x,h,t} \leq C_{\mathrm{POI},x,t} \forall (x,h,t) \quad (2)$$

where x indexes sites, h indexes hours, t indexes years, A is the available dispatchable energy [MW], C_{PV} and C_{wind} are the capacities of PV and wind [$MW_{nameplate}$], λ is the hourly availability of PV or wind [$MWh_{available}/MW_{nameplate}$], and C_{POI} is the POI capacity [MW_{POI}]. The dispatched energy D [$MWh_{dispatched}$] from site x is then limited by the available energy at that site:

$$D_{x,h,t} \leq A_{x,h,t} \forall (x,h,t) \quad (3)$$

As such, consistent with treating HPW generators as "full hybrids" [7] or "integrated hybrid resources" [34], we do not retain information on whether PV or wind at a given site x is being dispatched; all generation capacity "behind" the POI operates as a single plant with a combined availability profile $A_{x,h,t}$.

In baseline cases where hybridization is not allowed, an additional constraint is added forcing POI capacity at site x to be equal to the combined capacity of PV and wind at that site:

$$C_{\mathrm{POI},x,t} = C_{\mathrm{PV},x,t} + C_{\mathrm{wind},x,t} \forall (x,t) \quad (4)$$

In addition to the spur-line capex cost shown in Fig. 1a, spur-line capacity incurs a fixed operations & maintenance cost equal to 1.5% of upfront capex cost per year [35].

ReEDS also includes an estimate of intra-zonal network-reinforcement costs that may be required to move power from an HPW POI to demand centers within the model zone. Gorman et al. [36] report an average interconnection cost for fuel-based generators across the U.S. of $50/kW from 2005 to 2012, and an interconnection cost of $120/kW (a $70/kW difference) for renewable energy within MISO (through 2018)

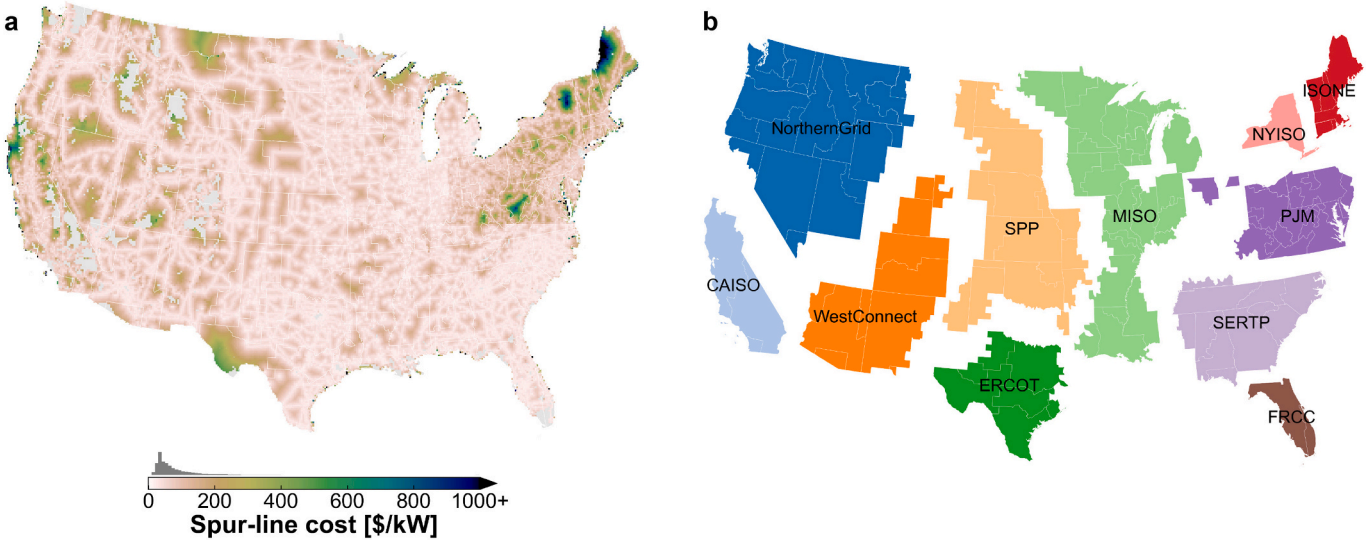

Fig. 1. Spur-line costs for new PV and wind plants and map of modeled regions. **a**, Spur-line costs for >56,000 grid cells across the contiguous US. The color bar includes a histogram of spur-line costs in $/kW; the unweighted average spur-line cost is 92 $/kW and the median is 57 $/kW. Not all sites shown here contain developable capacity for both PV and wind. **b**, Map of modeled "transmission regions" based on FERC order 1000 regions [32].

and PJM (through 2019), not including spur-line costs. Although there is substantial variability in these values across individual projects, in ReEDS we apply a uniform $50/kW cost to all increases in nameplate generation capacity by zone, plus an additional $70/kW cost to the site-specific spur-line capex cost shown in Fig. 1a. For HPW installations, these network-reinforcement costs apply to the POI capacity rather than the sum of PV and wind capacity, in the same manner as spur-line costs.

The Inflation Reduction Act of 2022 [37] gives PV installations the option of accepting the production tax credit (PTC) instead of the investment tax credit (ITC) and extends both tax credits through at least 2032. As written, the tax credits start to expire in either 2032 or the year in which electricity sector CO_2 emissions fall 75% below their level in 2022, whichever is later. Here, for simplicity, we assume the tax credits start to expire in 2032 and that PV and wind both utilize the PTC, which for HPW is applied to the total dispatched energy D of the HPW installation. Additional details regarding the representation of the Inflation Reduction Act in ReEDS are provided by Gagnon et al. [38].

2.2. Scenario assumptions

As noted above, we conduct independent system optimizations for each of the 11 transmission regions shown in Fig. 1b. All scenarios employ a declining CO_2 emissions constraint reaching zero direct power sector CO_2 emissions in 2040. The CO_2 cap follows a straight-line trajectory to zero, starting from historical 2018 emissions in the simulated transmission region, with the cap becoming active in 2025. To avoid double-counting, we do not enforce existing sub-national decarbonization policies including clean-energy standards, renewable portfolio standards, or the Regional Greenhouse Gas Initiative (RGGI).

Available generation and storage technologies include lithium-ion batteries, utility-scale PV, onshore wind, hydrogen (H_2) combustion turbines, hydropower, biopower, nuclear power, fossil gas combined cycle and combustion turbines, and coal, with modeling details given by Ho et al. [26]. Technologies other than utility-scale PV and onshore wind are modeled at the native 134-zone resolution of ReEDS. As in Cole et al. [27], the operation and electricity demand for H_2 production via electrolyzers is not explicitly modeled; instead, H_2 is assumed to be available at a price of 20 $/MMBtu. Electricity demand is modeled at the resolution of the 134 model zones and is assumed to follow the "high" trajectory from the NREL Electrification Futures Study [39–41]. Unless noted otherwise, cost and performance assumptions follow the moderate trajectories in the 2022 Annual Technology Baseline [42], and other model assumptions follow the Mid Case scenario in the 2022 Standard Scenarios report [38].

As noted above, the scenarios considered here employ much higher spatial and temporal resolution than typical simulations in ReEDS, increasing model size. In addition to running the model for 11 independent transmission regions as noted above, we also make the following simplifications to decrease computation time: concentrating solar power (CSP), offshore wind, and carbon capture & storage (CCS) technologies are excluded from the model; operating reserves are turned off; and the model is solved using 5-year time steps instead of the 2-year time steps typically used in ReEDS analyses.

2.3. Metrics

The "PV fraction" of HPW generation capacity installed at a particular site is given by C_{PV} / (C_{PV} + C_{wind}). PV capacities are given in DC terms (i.e. MW_{DC} or GW_{DC}) unless noted otherwise. To characterize the relative ratio of PV and wind at a given site, we introduce a "hybridization factor" denoted by ϕ:

$$\phi = \left|1 - 2\left|\frac{C_{PV}}{C_{PV} + C_{wind}} - \frac{1}{2}\right|\right| \tag{5}$$

The hybridization factor varies piecewise-linearly between 1 when $C_{PV} = C_{wind}$ and 0 when $C_{PV} = 0$ or $C_{wind} = 0$.

As noted in the Results and Discussion section, HPW plant capacity is given either as PV and wind nameplate capacity ($C_{PV} + C_{wind}$) or as POI capacity (C_{POI}). The generator-to-interconnection ratio (GIR) for a particular site is given by $GIR_{PV} = C_{PV} / C_{POI}$ or $GIR_{wind} = C_{wind} / C_{POI}$.

The net present value of projected system cost through 2040 is calculated using a discount rate of 5%. Other cost metrics are discussed in Ho et al. [26].

2.4. LCOE-minimizing hybrid designs

Our primary conclusions regarding the deployment and impacts of HPW are drawn from the electricity-system-cost-minimizing ReEDS CEM described above. To aid in the interpretation of these results, we separately utilize a simple site-LCOE-minimizing model to identify the GIR_{PV} and GIR_{wind} that minimize the LCOE for each modeled grid cell. The LCOE-minimizing model is defined as follows:

$$\begin{aligned}&\text{ANNUALCOST}\ [\$/\text{MWyear}]\\ &= (\text{CRF}_{PV} \bullet \text{CAPEXCOST}_{PV} + \text{FOMCOST}_{PV}) \bullet \text{GIR}_{PV}\\ &+(\text{CRF}_{wind} \bullet \text{CAPEXCOST}_{wind} + \text{FOMCOST}_{wind}) \bullet \text{GIR}_{wind}\\ &+\text{CRF}_{POI} \bullet \text{CAPEXCOST}_{POI} + \text{FOMCOST}_{POI}\end{aligned} \tag{6}$$

$$\text{CF}_h^{\text{unclipped}} = \text{GIR}^{PV} \bullet \text{CF}_h^{PV} + \text{GIR}^{wind} \bullet \text{CF}_h^{wind} \tag{7}$$

$$\text{CF}_h^{\text{total}} = \begin{cases} 1 \text{ if } \text{CF}_h^{\text{unclipped}} \geq 1 \\ \text{CF}_h^{\text{unclipped}} \text{ otherwise} \end{cases} \tag{8}$$

$$\text{LCOE}\ [\$/\text{MWh}] = \frac{\text{ANNUALCOST}}{\text{CF}_h^{\text{total}} \bullet 8760\text{hours}/\text{year}} - \text{PTC} \tag{9}$$

where CF_h^{total} is the hourly modeled capacity factor of the hybrid plant, CRF is the annual capital-recovery factor [fraction/year], CRF_{POI} is the GIR-weighted-average of CRF_{PV} and CRF_{wind}, $\bar{CF}_h^{total}$ is the average CF of the hybrid plant over 7 × 8760 h, CAPEXCOST is the upfront capital cost of generation capacity [$/MW], FOMCOST is the annual fixed operations and maintenance cost [$/MW-year], and ANNUALCOST is the total annualized plant cost [$/MW-year]. All numeric values are taken from ReEDS model inputs. The values of GIR_{PV} and GIR_{wind} that minimize LCOE are identified using the Nelder-Mead simplex algorithm [43], as implemented by the scipy.optimize.fmin() function in the SciPy Python package [44].

2.5. Caveats and limitations

To provide context for the interpretation of model results, we note the following caveats and limitations.

- Given the constraints and resolution of our linear CEM, we do not include all potential sources of value or cost-savings for hybrid systems. Other sources of value include the potential for reduced forecast uncertainty for HPW plants relative to standalone PV/wind plants, and the avoidance of operational constraints on maximum allowable ramp rates for independent VRE generators. Other potential cost-saving opportunities include reduced planning, permitting, or construction costs, or reduced project lead time if interconnection queues can be bypassed in situations where PV capacity is added to an existing wind site without increasing the POI capacity.
- ReEDS includes site-level variation in spur-line costs (Fig. 1a), but intra-zone network reinforcement costs use a spatially-uniform per-kW cost adder. As discussed by Gorman et al. [36], network reinforcement costs exhibit substantial regional variation. Including a geographically resolved estimate of network reinforcement costs could change the spatial patterns of VRE deployment within and across model zones.

- The firm capacity provided by HPW installations toward meeting the planning-reserve margin is taken as the sum of the nameplate capacities of PV and wind multiplied by the PV and wind capacity credits (calculated independently as described by Ho et al. [26]) and is not adjusted for site POI capacity. As the majority of firm capacity is provided by resources other than PV and wind in these scenarios, this simplification is not expected to substantially impact the results.
- All PV systems are modeled with an inverter-loading ratio (ILR) of 1.3, approximating recent industry trends [45]. For sites with an optimal $GIR_{PV} > 1.3$, increasing the ILR by decreasing the inverter capacity to match the POI capacity would provide additional cost savings.
- CSP, offshore wind, and CCS are not included given their currently small contribution to generation capacity nationwide and the need to simplify other aspects of the model to enable the higher spatial and temporal resolution required for this study of land-based HPW. This modeling decision does not imply a judgment about the suitability of these other technologies for hybridization or future expansion.
- As noted above, as we model each FERC region in isolation, we do not include transmission flows between FERC regions in this analysis (although transmission expansion and flows between ReEDS zones *within* FERC regions are modeled as usual). While other studies have demonstrated large potential benefits from interregional coordination and transmission expansion [46], interregional transmission currently represents a small fraction of regional firm capacity plans (≤6% of regional demand by NERC region in 2024 [47]), and it is sometimes excluded in other analyses of the United States [48–50]. Computational advancements (or simplification of other model dimensions) would be required to represent interregional transmission concurrently with the high spatial and temporal resolution used here and should be explored in future work.
- While we include standalone energy storage (represented by lithium-ion batteries and pumped hydro, where appropriate) at 134-zone resolution, to reduce computational complexity we do not model hybridization of storage with PV or wind in this work. Previous work has shown that PV + battery hybrids can be competitive in a least-cost optimization framework, particularly in decarbonized systems; however, the simulated deployment of PV + battery hybrids largely displaces that of standalone PV and battery capacity, and hybridization with storage does not significantly change the generation mix or total electricity system cost [51].

3. Results and discussion

3.1. Where is HPW capacity deployed?

Fig. 2 shows the spatial distribution of PV and wind deployment through 2040 with and without the ability to hybridize (i.e., share POI capacity and costs) across the 11 modeled transmission regions; Fig. 3 provides a zoomed-in view of ERCOT to more clearly illustrate the differences between the two scenarios. Note that because the spatial density of available capacity [MW/km^2] is ~10× higher for PV than for wind (where the wind capacity density is defined over an entire wind installation, including inter-turbine spacing), a single 11.5 km × 11.5 km grid cell can host up to ~4000 MW of PV capacity and up to ~400 MW of wind capacity. To facilitate comparison between technologies, the color scale in Fig. 2 and Fig. 3 peaks at 400 MW for both PV and wind.

Allowing hybridization does not noticeably affect the spatial patterns of wind deployment in the modeled regions. Differences associated with hybridization are more pronounced for PV, primarily within the "wind belt" regions (SPP, ERCOT, and MISO) but to some extent in all regions. A spatial shift in capacity deployment with spur-line sharing indicates a situation where the model forgoes deployment at the "best" standalone site (where "best" includes the combined effects of resource quality, generator and POI cost, and value of the energy, firm capacity, and

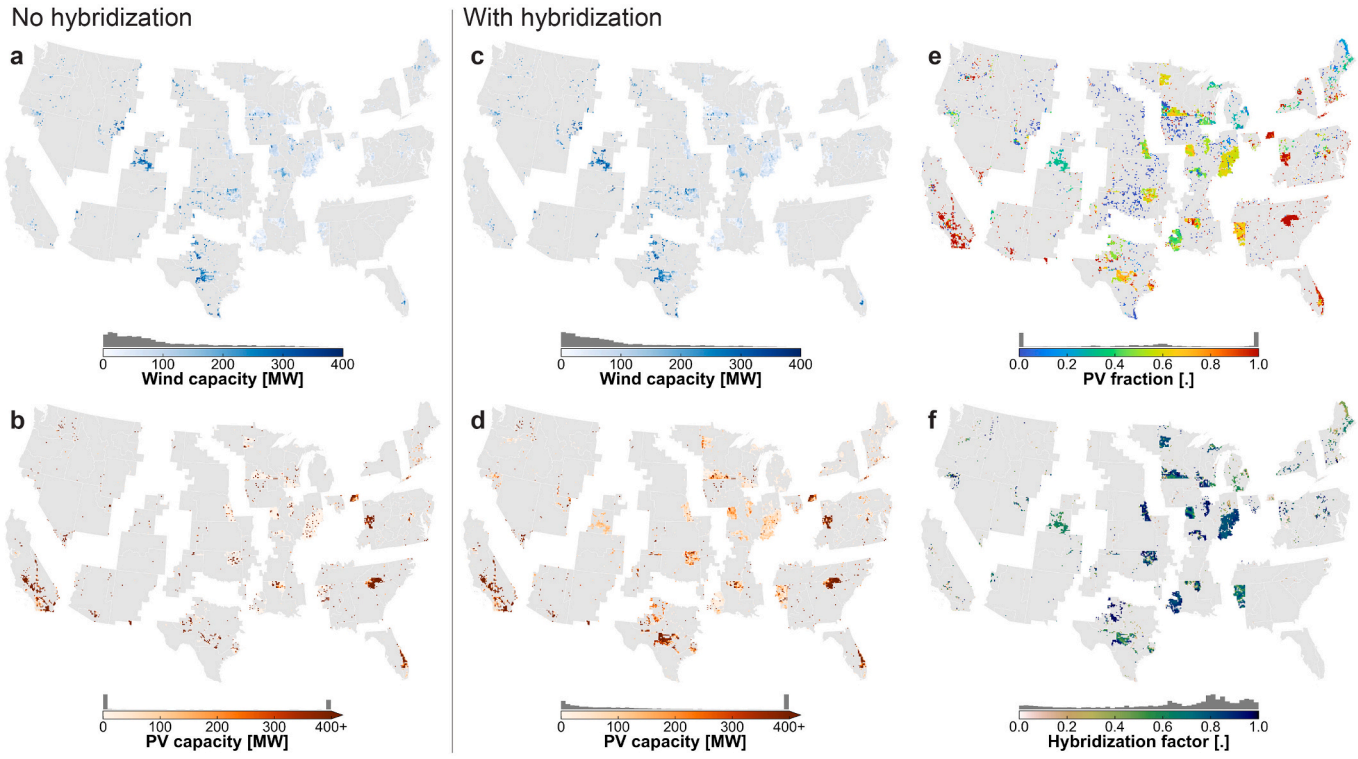

Fig. 2. Modeled PV and wind capacity in 2040 across the 11 modeled transmission regions. **a**,**b**, Maps of wind (**a**) and PV (**b**) capacity for scenarios without hybridization (i.e. shared POI capacity and costs). **c**,**d**, Maps of wind (**c**) and PV (**d**) capacity for scenarios with hybridization. **e**, Map of the PV fraction for all sites with PV and/or wind capacity when spur-line sharing is allowed. **f**, Map of the "hybridization factor" ϕ for all sites with PV and wind capacity. Sites with a hybridization factor of zero (i.e. wind-only or PV-only sites) are excluded from **f** for clarity. All results are for scenarios that reach zero electricity-sector CO_2 emissions in 2040.

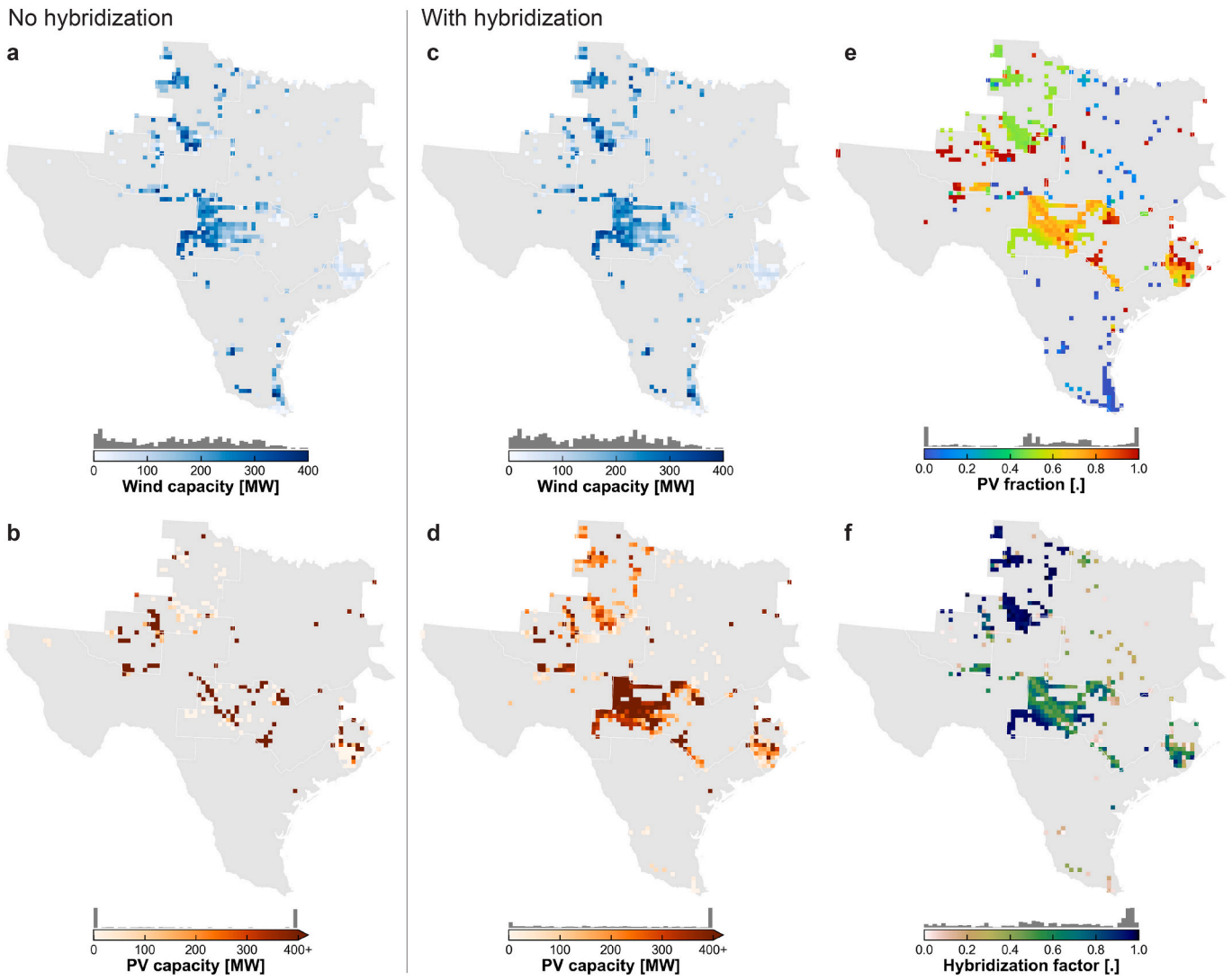

Fig. 3. Modeled PV and wind capacity in 2040 for the ERCOT region. Values are the same as in Fig. 2. **a**,**b**, Maps of wind (**a**) and PV (**b**) capacity for scenarios without hybridization (i.e. shared POI capacity and costs). **c**,**d**, Maps of wind (**c**) and PV (**d**) capacity for scenarios with hybridization. **e**, Map of the PV fraction for sites in ERCOT with PV and wind capacity when spur-line sharing is allowed. **f**, Map of the "hybridization factor" ϕ for sites in ERCOT with PV and wind capacity. Sites with a hybridization factor of zero (i.e. wind-only or PV-only sites) are excluded from **f** for clarity. All results are for scenarios that reach zero electricity-sector CO_2 emissions in 2040.

emissions reductions provided) and instead deploys capacity at a site where POI capacity and cost can be shared with the other resource type. As can be seen most clearly in ERCOT (Fig. 3), when hybridization is allowed, some PV capacity shifts from highly concentrated standalone PV sites to sites where wind capacity, and associated POI capacity, is deployed.

Two factors likely explain why PV capacity is more likely to shift to wind sites than vice versa. First, wind resource quality varies more widely with location than PV resource quality; modeled wind capacity factor varies by a factor of ~5.6× between the windiest and least-windy site, while PV capacity factor varies by a factor of ~2.1× between the sunniest and least-sunny site (Fig. A 1 in the Supplemental Information). A PV installation is therefore less likely to sacrifice a large amount of annual energy production potential by relocating from the "best" standalone solar site in a given model zone to a site with wind capacity and associated sharable POI capacity; relocating a wind installation to a PV site would be more likely to incur a larger sacrifice in wind resource quality. Second, the ~10× lower capacity density of wind means that for a given quantity of generation capacity, ~10× more sites would be occupied by wind than PV. There are therefore more options for adding PV to a standalone wind site than vice versa.

The total amount of PV and wind capacity deployed across all regions by 2040 when hybridization is allowed is shown in Fig. 4, quantified in terms of POI capacity (Fig. 4a) and behind-the-POI nameplate PV + wind capacity (Fig. 4b) as a function of the optimized hybridization factor. The majority of installations do not employ significant hybridization: 740 GW of POI capacity (out of 1290 GW total) are deployed at sites with a hybridization factor <0.05, i.e. with a site PV:wind capacity ratio <1:39 or >39:1.

Hybrid deployment is nevertheless significant. The cost-optimal solution includes 290 GW of POI capacity with a hybridization factor >0.5 (i.e., with a site PV/wind capacity ratio between 1:3 and 3:1), 70% (or 210 GW) of which is installed in the "wind belt" regions of SPP, ERCOT, and MISO. The corresponding behind-the-POI PV and wind nameplate capacity totals 540 GW; for context, the combined nameplate capacity of PV (DC) and wind installed across the US at the end of 2020 was ~220 GW [52,53].

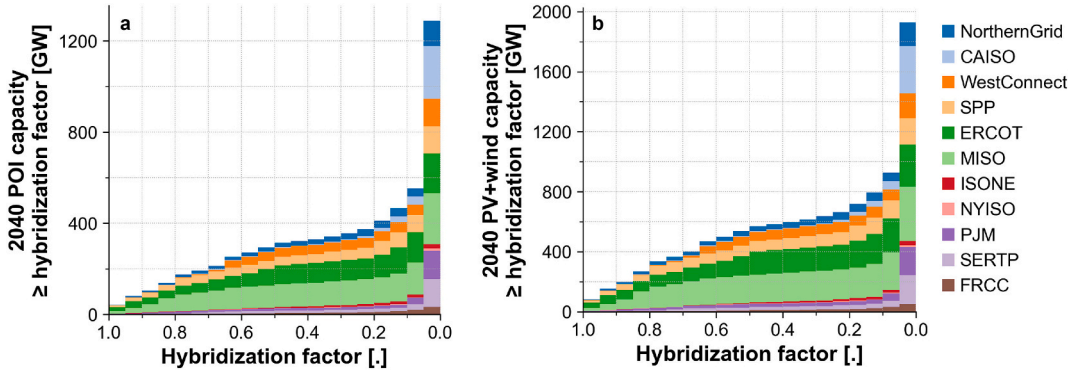

Fig. 4. HPW capacity in 2040 across modeled regions, sorted by hybridization factor. Bars indicate installed capacity with hybridization factor greater than or equal to the corresponding x-axis value. **a**, HPW capacity quantified in terms of POI (spur-line) capacity. **b**, HPW capacity quantified in terms of the sum of "behind-the-POI" PV and wind nameplate capacity. PV nameplate capacity is in GW_{DC}.

3.2. What drives HPW deployment?

To elucidate the drivers of HPW deployment, we include the results of a simple model that identifies the GIR_{PV} and GIR_{wind} that minimize the LCOE for each grid cell containing nonzero developable capacity for both wind and PV. The results of this model are shown in **Fig. 5**a-c for input assumptions consistent with the corresponding ReEDS scenario assumptions in 2025. When the results of the LCOE-minimizing model are plotted as a function of the PV LCOE and wind LCOE (Fig. 5c), a particularly simple trend is evident: hybrids tend to be the LCOE-minimizing choice in regions where the LCOEs of standalone PV and standalone wind are roughly equivalent—i.e. along the boundary between low-cost-wind and low-cost-PV regions. For sites where spur-line costs are low (the leftmost subplots of Fig. 5c), hybrids are only optimal when the PV and wind LCOEs are very nearly equal; for sites with higher spur-line cost (the rightmost subplot of Fig. 5c), there is more incentive to overbuild generation capacity relative to POI capacity, and more room for hybridization to reduce LCOE even when one resource is substantially cheaper than the other.

Of course, as is widely noted in the literature [54,55], LCOE is insufficient for assessing the economic competitiveness of an investment in generation capacity, primarily because it does not capture the time-varying value of electricity services (including energy, firm capacity, and emissions policy value) or the impact of siting constraints on capacity deployment. The ReEDS CEM results for installed capacity in 2040 (Fig. 5d) share some rough similarities with the LCOE-minimizing results—where standalone wind tends to be installed at low-wind-LCOE sites, standalone PV tends to be installed at low-PV-LCOE sites, and HPW tends to be deployed at sites with low and similar PV and wind LCOEs—but there are many exceptions. Standalone wind capacity is sometimes installed at sites where the LCOE of PV is lower than that of wind, and vice versa; there are also many lower-LCOE sites passed over in favor of higher-LCOE sites where the overall system value (i.e. the reduction in total system cost) is higher. The same behavior is also observed if deployment is assessed at the level of individual transmission regions (Fig. A 2 in the Supplemental Information).

Some of the deviation from LCOE-minimizing deployment is related to the cumulative nature of deployed capacity; the 2040 capacity shown in Fig. 5 and Fig. A 2 includes all non-retired capacity built in previous model years, and the relative competitiveness of PV and wind changes over time and across different regions according to their relative costs and the evolving profile of different categories of system value on the path to zero carbon in 2040. Wind capacity and associated spur-line capacity may be installed at a given site in 2030 to provide energy, capacity, or emissions-reduction value; in 2035, that site becomes more attractive for PV capacity because its spur line is already installed and paid for (in contrast to the LCOE-minimizing model which only considers "greenfield" investments).

In sum, we observe that while a site-LCOE-minimizing model indicates a particularly simple correspondence between PV LCOE, wind LCOE, spur-line cost, and optimal HPW deployment, HPW deployment patterns identified by a system-cost-minimizing CEM are considerably more complex, capturing the combined effects of energy/capacity/emissions value, brownfield spur-line capacity, local siting and transmission constraints, and the time-varying evolution of wind and solar cost and performance.

3.3. What value does hybridization provide in a CEM?

To explore the impact of hybrid deployment on the overall electricity system, Fig. 6 shows total system cost, POI capacity, generation capacity, hybridization factors, and GIRs from the ReEDS CEM for 2040 summed over the 11 transmission regions. To address uncertainty in estimated interconnection costs, results for three different POI cost assumptions (1×, 2×, and 5× multipliers on the spur-line costs shown in Fig. 1a and reinforcement costs discussed in Section 2.1.3) are shown for each metric.

The net present value of system cost savings resulting from hybridization through 2040 (Fig. 6a) amounts to $40 billion (0.8%) in the "1× POI cost" case, $60 billion (1.3%) in the "2× POI cost" case, and $90 billion (1.9%) in the "5× POI cost" case. Allowing hybridization reduces new spur-line capacity by ~8% in the 1× POI cost case and <2% in the 2× and 5× POI cost cases.

Allowing hybridization increases solar capacity by 50–110 GW and wind capacity by 25–75 GW depending on the POI cost assumption, but otherwise does not qualitatively alter the overall capacity mix; in the central POI cost case, PV and wind constitute the majority of installed capacity with and without hybridization, supplemented by smaller amounts of battery storage, hydrogen combustion turbines, and nuclear. The 2× and 5× POI cost scenarios utilize less solar, wind, and storage capacity and a greater amount of nuclear capacity. As expected, site hybridization factors and generator:inverter ratios increase as POI costs increase (Fig. 6d-e): the median hybridization factor increases from 0.75 to 0.85 from 1× POI to 5× POI and the median GIR increases from 1.6 to 2.2.

4. Conclusions

The results described here suggest that, from the point of view of a system planner under zero-carbon conditions, the primary impact of allowing PV-wind hybridization is spatial: when hybridization is allowed, some PV capacity tends to be relocated from standalone sites to sites where wind has previously or is currently being deployed, and where POI capacity can be shared (Fig. 2 and Fig. 3). This change is

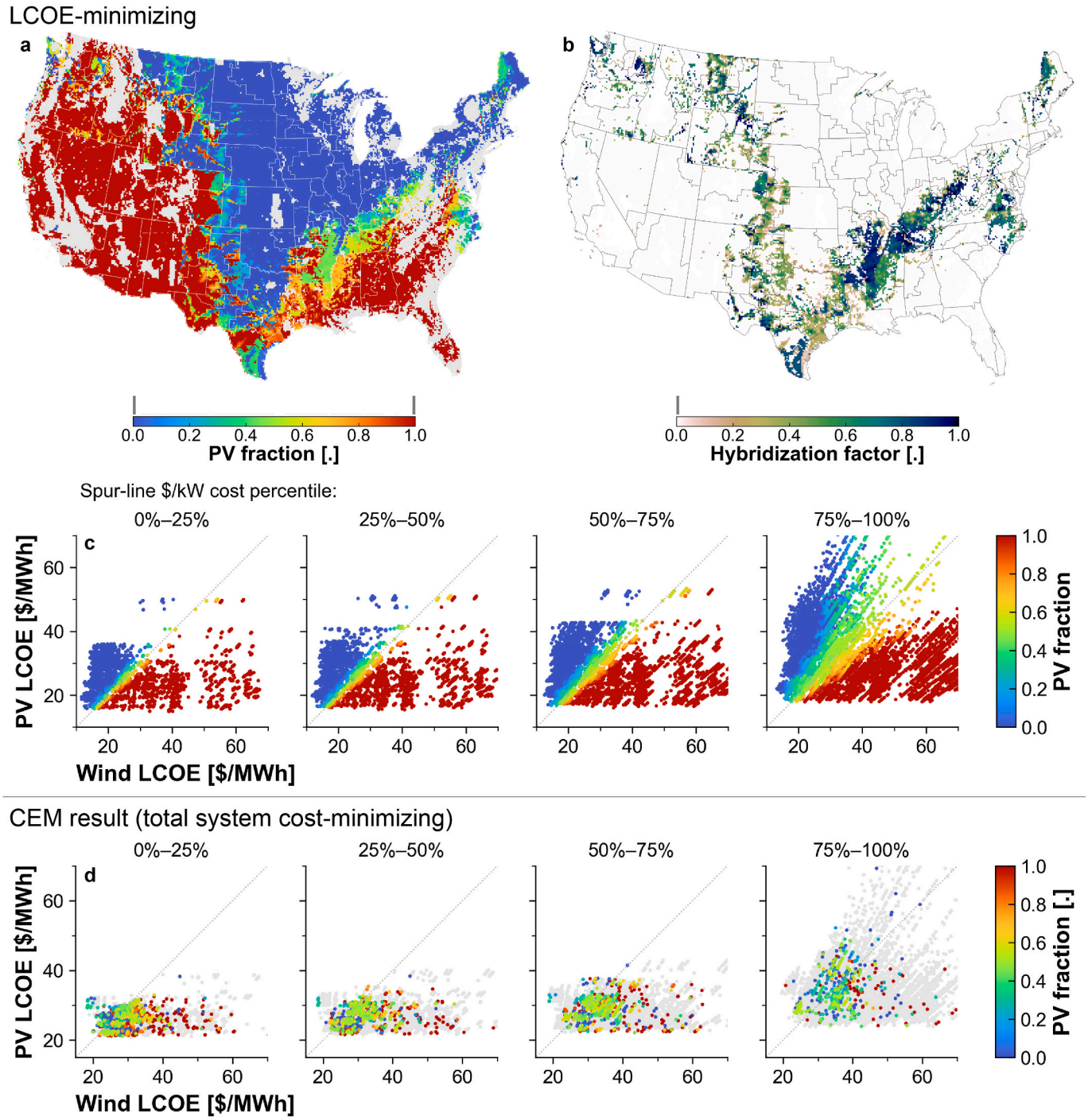

Fig. 5. Results of a site-LCOE-minimizing model compared to the results of the electricity-system-cost-minimizing CEM. **a**, PV fraction by site across the US for the site-LCOE-minimizing model under 2025 cost assumptions. **b**, Hybridization factor by site across the US for the site-LCOE-minimizing model. **c**, PV fraction by site for the site-LCOE-minimizing model as a function of GIR-optimized standalone PV LCOE by site (y axis), GIR-optimized standalone wind LCOE by site (x axis), and spur-line cost quartile (four panels). Hybrid plants (PV fraction between 0 and 1, non-inclusive) are primarily clustered along the $LCOE_{PV} = LCOE_{wind}$ line for sites in the first three spur-line cost quartiles. The spur-line cost quartile cutoffs are 128, 154, and 207 $/kW. **d**, PV fraction by site for the results of the electricity-system-cost-minimizing CEM for 2040, presented in the same format as **c**. Panel **d** uses 2040 cost assumptions; gray points indicate sites not chosen for investment and colored points indicate sites with nonzero installed capacity in the optimized solution. LCOE values in **d** use a GIR of 1 for both PV and wind.

accompanied by an ~8% reduction in spur-line TW-miles required for PV and wind interconnection under central cost assumptions, contributing to overall system cost savings of 0.8% (or up to 1.9% in scenarios with higher interconnection costs) (Fig. 6). Hybrid deployment does not always represent the LCOE-minimizing design on a site-by-site basis (Fig. 4), instead reflecting the combined effects of local costs, local energy, capacity, and emissions-reduction values, and the impact of existing transmission capacity.

For a system planner, the relevant comparison is not between HPW and standalone wind at a single site, or HPW and standalone PV at a single site, but between the cost-optimal portfolio of PV, wind, and transmission capacity with and without hybridization. Compared to

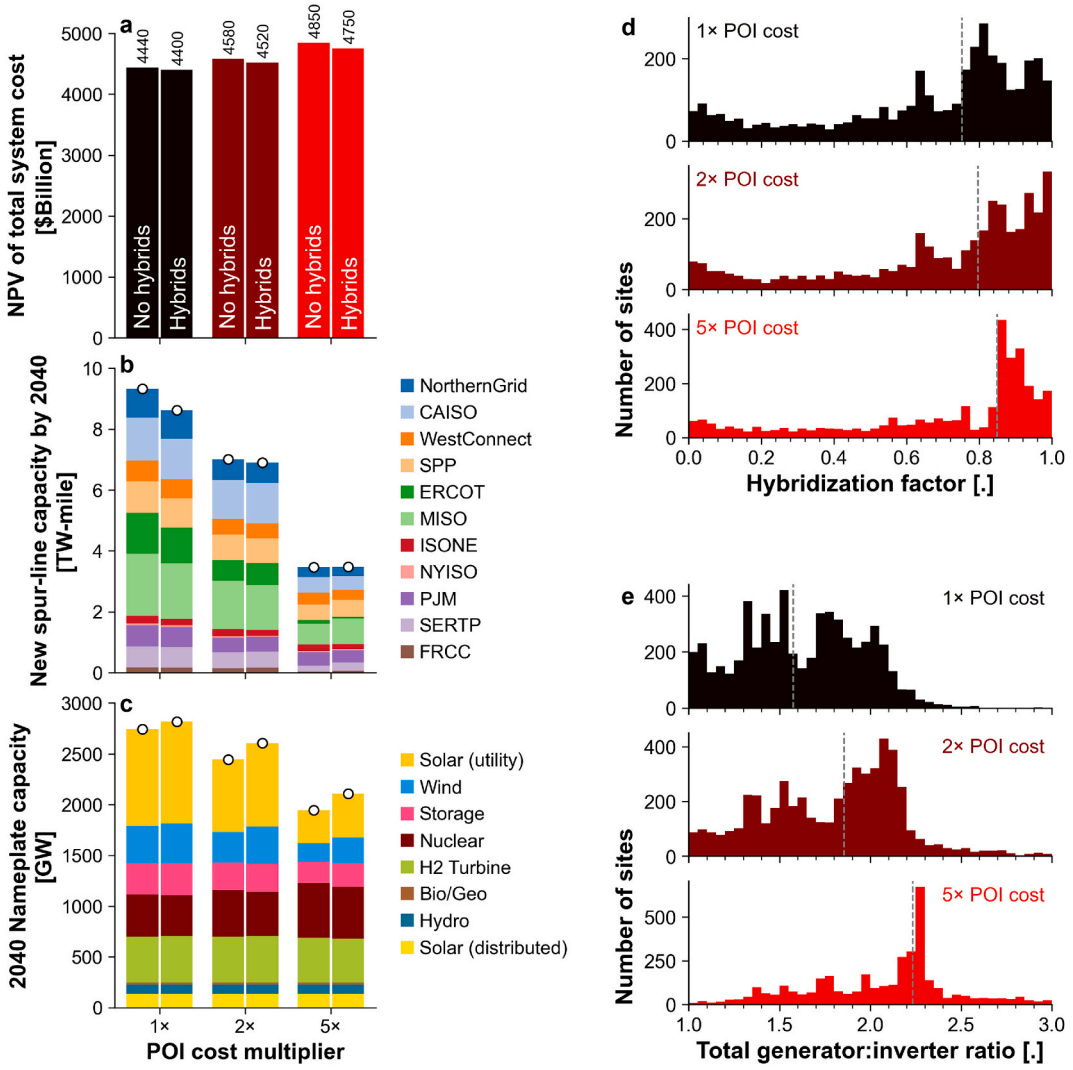

Fig. 6. CEM results for 2040 summed over the 11 transmission regions. **a**, Net present value (NPV) of 2022–2040 system cost; **b**, new spur-line capacity through 2040 by transmission region; **c**, 2040 generation capacity by technology. The left bar in each pair shows results without hybridization and the right bar shows results with hybridization; the three pairs indicate POI cost multipliers of 1×, 2×, and 5× from left to right. **d**, Histograms of site hybridization factors across all transmission regions for three POI cost multipliers; **e**, histograms of site GIRs under the same conditions. All results are for scenarios that reach zero electricity-sector CO_2 emissions in 2040.

independent wind and PV installations with no "overbuilding" of generation capacity relative to POI capacity, hybridization via interconnection-sharing can only decrease the combined capacity factor and annual energy production potential. But in locations with high interconnection costs, the savings that result from interconnection capacity sharing can outweigh the reduction in capacity factor and lead to overall system cost savings.

Future work could address additional potential sources of hybrid value beyond those addressed here, including the ability to co-locate energy storage or electrolyzers for hydrogen production alongside PV or wind capacity behind the POI to utilize excess energy that would otherwise be clipped by the interconnection capacity. Our results indicate that interconnection cost assumptions are a particularly important driver of hybrid deployment (Fig. 6). Improving the representation and spatial resolution of these costs in CEMs should therefore be a priority in further work on hybrid resources.

CRediT authorship contribution statement

Patrick R. Brown: Writing – review & editing, Writing – original draft, Visualization, Software, Methodology, Investigation, Formal analysis, Conceptualization. **Travis Williams:** Resources, Data curation. **Maxwell L. Brown:** Software. **Caitlin Murphy:** Writing – review & editing, Supervision, Project administration, Funding acquisition, Conceptualization.

Declaration of competing interest

The authors declare that they have no known competing financial interests or personal relationships that could have appeared to influence the work reported in this paper.

Data availability

The ReEDS model and data are available open source at https://github.com/NREL/ReEDS-2.0

Acknowledgments

The authors acknowledge T. Mai, A. Lopez, M. Schwartz, W. Cole, A. Bloom, D. Palchak, J. Cochran, and the members of the ReEDS team for helpful discussions and feedback. This work was authored by the

National Renewable Energy Laboratory, operated by the Alliance for Sustainable Energy, LLC, for the U.S. Department of Energy (DOE) under contract no. DE-AC36-08GO28308. Funding was provided by the U.S. Department of Energy Office of Energy Efficiency and Renewable Energy Strategic Analysis Team and Wind Energy Technologies Office. The views expressed in the article do not necessarily represent the views of the DOE or the U.S. Government. The U.S. Government retains and the publisher, by accepting the article for publication, acknowledges that the U.S. Government retains a nonexclusive, paid-up, irrevocable, worldwide license to publish or reproduce the published form of this work, or allow others to do so, for U.S. Government purposes.

Appendix A. Supplementary data

Supplementary data to this article can be found online at https://doi.org/10.1016/j.apenergy.2024.123151.

References

[1] Bistline JET. Roadmaps to net-zero emissions systems: emerging insights and modeling challenges. Joule 2021;5(10):2551–63. https://doi.org/10.1016/j.joule.2021.09.012.
[2] Breyer C, Khalili S, Bogdanov D, Ram M, Oyewo AS, Aghahosseini A, et al. On the history and future of 100% renewable energy systems research. IEEE Access 2022;10(June):78176–218. https://doi.org/10.1109/ACCESS.2022.3193402.
[3] Denholm P, Brown P, Cole W, Mai T, Sergi B, Brown M, et al. Examining Supply-Side Options to Achieve 100% Clean Electricity by 2035. NREL/TP-6A40–81644. Sep. 2022. https://doi.org/10.2172/1885591.
[4] Seel J, Kemp JM, Rand J, Gorman W, Millstein D, Kahrl F, et al. Generator interconnection costs to the transmission system. Lawrence Berkeley National Laboratory; 2023. https://emp.lbl.gov/publications/generator-interconnection-costs.
[5] Rand J, Strauss R, Gorman W, Seel J, Kemp JM, Jeong S, et al. Queued up: Characteristics of power plants seeking transmission interconnection as of the end of 2022. Accessed: Dec. 01, 2023, https://emp.lbl.gov/queues; Apr. 2023.
[6] International Energy Agency (IEA). Electricity grids and the energy transition. International Energy Agency (IEA); 2023. https://www.iea.org/reports/electricity-grids-and-secure-energy-transitions.
[7] Murphy CA, Schleifer A, Eurek K. A taxonomy of systems that combine utility-scale renewable energy and energy storage technologies. Renew Sustain Energy Rev 2021;139, no. January:110711. https://doi.org/10.1016/j.rser.2021.110711.
[8] Wind Europe. Database for wind + storage co-located projects. https://windeurope.org/about-wind/database-for-wind-and-storage-colocated-projects/.
[9] Weschenfelder F, de Novaes Pires G, Leite AC, Araújo da Costa O, de Castro Vilela CM, Ribeiro AA, et al. A review on the complementarity between grid-connected solar and wind power systems. J Clean Prod 2020;257:120617. https://doi.org/10.1016/j.jclepro.2020.120617.
[10] Stenclik D, Goggin M, Ela E, Ahlstrom M. Unlocking the flexibility of hybrid resources. Energy Systems Integration Group; 2022. https://www.esig.energy/wp-content/uploads/2022/03/ESIG-Hybrid-Resources-report-2022.pdf.
[11] Bolinger M, Gorman W, Rand J, Wiser R, Jeong S, Seel J, et al. Hybrid power plants: Status of operating and proposed plants, 2022 edition. Lawrence Berkeley National Laboratory; 2022. https://emp.lbl.gov/sites/default/files/hybrid_plant_tracking_2022_0.pdf.
[12] U.S. Federal Energy Regulatory Commission. Order 845 - Reform of Generator Interconnection Procedures and Agreements. US Federal Energy Regulatory Commission; 2018. https://www.ferc.gov/sites/default/files/2020-06/Order-845.pdf.
[13] Lindberg O, Arnqvist J, Munkhammar J, Lingfors D. Review on power-production modeling of hybrid wind and PV power parks. J Renew Sustain Energy 2021;13(4). https://doi.org/10.1063/5.0056201.
[14] Khare V, Nema S, Baredar P. Solar-wind hybrid renewable energy system: a review. Renew Sustain Energy Rev 2016;58:23–33. https://doi.org/10.1016/j.rser.2015.12.223.
[15] Ganguly P, Kalam A, Zayegh A. Solar-wind hybrid renewable energy system: current status of research on configurations, control, and sizing methodologies. Elsevier Ltd; 2018. https://doi.org/10.1016/B978-0-08-102493-5.00012-1.
[16] Costoya X, Carvalho D. Assessing the complementarity of future hybrid wind and solar photovoltaic energy resources for North Americavol. 173; 2023. p. 113101. https://doi.org/10.1016/j.rser.2022.113101. no. October 2022.
[17] Harrison-Atlas D, Murphy C, Schleifer A, Grue N. Temporal complementarity and value of wind-PV hybrid systems across the United States. Renew Energy 2022;201(P1):111–23. https://doi.org/10.1016/j.renene.2022.10.060.
[18] Manocha, A., Patankar, N., Jenkins, J.D. Reducing transmission expansion by co-optimizing sizing of wind, solar, storage and grid connection capacity. arXiv, Mar 2023. https://arxiv.org/abs/2303.11586.
[19] Kapica J, Canales FA, Jurasz J. Global atlas of solar and wind resources temporal complementarity. Energ Conver Manage 2021;246, no. September:114692. https://doi.org/10.1016/j.enconman.2021.114692.
[20] Jurasz J, Canales FA, Kies A, Guezgouz M, Beluco A. A review on the complementarity of renewable energy sources: Concept, metrics, application and future research directions. Solar Energy 2020;195(April 2019):703–24. https://doi.org/10.1016/j.solener.2019.11.087.
[21] Aquila G, Souza Rocha LC, de Oliveira Pamplona E, de Queiroz AR, Rotela Junior P, Balestrassi PP, et al. Proposed method for contracting of wind-photovoltaic projects connected to the Brazilian electric system using multiobjective programming. Renew Sustain Energy Rev 2018;97(May):377–89. https://doi.org/10.1016/j.rser.2018.08.054.
[22] Aquila G, de Queiroz AR, Rotela Junior P, Rocha LCS, de Pamplona EO, Balestrassi PP. Contribution for bidding of wind-photovoltaic on grid farms based on NBI-EFA-SNR method. Sustain Energy Technol Assess 2020;40, no. May:100754. https://doi.org/10.1016/j.seta.2020.100754.
[23] Carvalho DB, Guardia EC, Marangon Lima JW. Technical-economic analysis of the insertion of PV power into a wind-solar hybrid system. Solar Energy 2019;191(September):530–9. https://doi.org/10.1016/j.solener.2019.06.070.
[24] Yendaluru RS, Karthikeyan G, Jaishankar A, Babu S. Techno-economic feasibility analysis of integrating grid-tied solar PV plant in a wind farm at Harapanahalli, India. Environ Prog Sustain Energy 2020;39(3):1–10. https://doi.org/10.1002/ep.13374.
[25] De Azevedo R, Mohammed O. Profit-maximizing utility-scale hybrid wind-PV farm modeling and optimization. In: *Conference Proceedings - IEEE SOUTHEASTCON*, vol. 2015-June; June, 2015. https://doi.org/10.1109/SECON.2015.7132892.
[26] Ho J, Becker J, Brown M, Brown P, Chernyakhovskiy I, Cohen S, et al. Regional Energy Deployment System (ReEDS) Model Documentation: Version 2020. *National Renewable Energy Laboratory (NREL)*; 2021. June, https://www.nrel.gov/docs/fy21osti/78195.pdf.
[27] Cole WJ, Greer D, Denholm P, Frazier AW, Machen S, Mai T, et al. Quantifying the challenge of reaching a 100% renewable energy power system for the United States. Joule Jul 2021;5(7):1732–48. https://doi.org/10.1016/j.joule.2021.05.011.
[28] Gates N, Cole W, Frazier A, Gagnon P. Evaluating the Interactions Between Variable Renewable Energy and Diurnal Storage. National Renewable Energy Laboratory; Oct 2021. https://doi.org/10.2172/1827634. NREL/TP-6A20-78042.
[29] Brown M, Irish M, Steinberg D, Chanpiwat P. Considerations for Temporal Representation in Electricity Capacity Expansion Modeling (in prep). National Renewable Energy Laboratory; 2022.
[30] Maclaurin G, Grue N, Lopez A, Heimiller D. The Renewable Energy Potential (reV) Model: A Geospatial Platform for Technical Potential and Supply Curve Modeling. National Renewable Energy Laboratory; 2019. https://www.nrel.gov/docs/fy19osti/73067.pdf.
[31] Lopez A, Pinchuk P, Gleason M, Cole W, Mai T, Williams T, et al. Solar Photovoltaics and Land-Based Wind Technical Potential and Supply Curves for the Contiguous United States: 2023 Edition. National Renewable Energy Laboratory; 2024. NREL/TP-6A20–87843, https://www.nrel.gov/docs/fy24osti/87843.pdf.
[32] U.S. Federal Energy Regulatory Commission. Order No. 1000 - Transmission planning and cost allocation. Accessed: Mar. 25, 2022, https://www.ferc.gov/electric-transmission/order-no-1000-transmission-planning-and-cost-allocation; 2021.
[33] U.S. Department of Energy. National Transmission Needs Study. https://www.energy.gov/gdo/national-transmission-needs-study; 2023.
[34] Federal Energy Regulatory Commission (FERC). Hybrid Resources White Paper. White Paper AD20–9–000, https://www.ferc.gov/media/hybrid-resources-white-paper.
[35] Joint Research Centre of the European Commission. Energy Technology Reference Indicator projections for 2010-2050. Joint Research Centre of the European Commission; 2014. https://doi.org/10.2790/057687.
[36] Gorman W, Mills A, Wiser R. Improving estimates of transmission capital costs for utility-scale wind and solar projects to inform renewable energy policy. Energy Policy 2019;135(September):110994. https://doi.org/10.1016/j.enpol.2019.110994.
[37] Yarmuth JA. *H.R.5376 - Inflation Reduction Act of* 2022. https://www.congress.gov/bill/117th-congress/house-bill/5376/text; 2022.
[38] Gagnon P, Brown Maxwell, Steinberg Dan, Brown Patrick, Awara Sarah, Carag Vincent, et al. 2022 Standard Scenarios Report: A U.S. Electricity Sector Outlook. National Renewable Energy Laboratory; Dec. 2022. NREL/TP-6A40-84327, https://www.nrel.gov/docs/fy23osti/84327.pdf.
[39] Mai TT, Jadun P, Logan JS, McMillan CA, Muratori M, Steinberg DC, et al. Electrification futures study: Scenarios of electric technology adoption and power consumption for the United States. Golden, CO: National Renewable Energy Laboratory; Jun. 2018. https://doi.org/10.2172/1459351. NREL/TP-6A20-71500.
[40] Mai T, Jadun P, Logan J, McMillan C, Muratori M, Steinberg D, et al. Electrification Futures Study Load Profiles. https://data.nrel.gov/submissions/126.
[41] Sun Y, Paige J, Brent N, Matteo M, Caitlin M, Logan J, et al. Electrification Futures Study: Methodological Approaches for Assessing Long-Term Power System Impacts of End-Use Electrification. Technical Report NREL/TP-6A20–73336. Jul. 2020.
[42] National Renewable Energy Laboratory. Annual Technology Baseline 2022. https://atb.nrel.gov/electricity/2022/data.
[43] Nelder JA, Mead R. A simplex method for function minimization. Computer J Jan 1965;7(4):308–13. https://doi.org/10.1093/comjnl/7.4.308.
[44] Virtanen P, Gommers R, Oliphant TE, Haberland M, Reddy T, Cournapeau D, et al. SciPy 1.0: fundamental algorithms for scientific computing in Python. Nat Methods 2020;17(3):261–72. https://doi.org/10.1038/s41592-019-0686-2.
[45] Bolinger M, Seel J, Warner C, Robson D. Utility-scale solar, 2021 edition. Lawrence Berkeley National Laboratory; 2021. https://emp.lbl.gov/sites/default/files/utility_scale_solar_2021_edition_slides.pdf.

[46] Brown PR, Botterud A. The value of inter-regional coordination and transmission in decarbonizing the US electricity system. Joule Dec 2020;5(1):115–34. https://doi.org/10.1016/j.joule.2020.11.013.
[47] North American Electric Reliability Corporation. 2023 Long-term reliability assessment. North American Electric Reliability Corporation; 2023. https://www.nerc.com/pa/RAPA/ra/Reliability%20Assessments%20DL/NERC_LTRA_2023.pdf.
[48] Larson E, Greig C, Jenkins J, Mayfield E, Pascale A, Zhang C, et al. Net-zero America: Potential pathways, infrastructure, and impacts, final report. Princeton, NJ: Princeton University; 2021. https://www.dropbox.com/s/ptp92f65lgds5n2/Princeton%20NZA%20FINAL%20REPORT%20%2829Oct2021%29.pdf?dl=0.
[49] Sepulveda NA, Jenkins JD, Edington A, Mallapragada DS, Lester RK. The design space for long-duration energy storage in decarbonized power systems. Nat Energy May 2021;6(5):506–16. https://doi.org/10.1038/s41560-021-00796-8.
[50] Ziegler MS, Mueller JM, Pereira GD, Song J, Ferrara M, Chiang Y-M, et al. Storage requirements and costs of shaping renewable energy toward grid decarbonization. Joule Sep 2019;3(9):2134–53. https://doi.org/10.1016/j.joule.2019.06.012.
[51] Murphy C, Brown P, Carag V. The Roles and Impacts of PV-Battery Hybrids in a Decarbonized U.S. Electricity Supply. National Renewable Energy Laboratory; Sep 2022. https://doi.org/10.2172/1887559. NREL/TP-6A40-82046.
[52] Feldman D, Margolis R. H2 2020: Solar Industry Update. National Renewable Energy Laboratory; 2021. https://www.nrel.gov/docs/fy21osti/79758.pdf.
[53] Wiser R, Bolinger M, Hoen B, Millstein D, Rand J, Barbose G, et al. Land-based wind market report: 2021 edition. U.S. Department of Energy; 2021. http://www.osti.gov.
[54] Joskow PL. Comparing the costs of intermittent and dispatchable electricity generating technologies. Am Econ Rev 2011;101(3):238–41. https://doi.org/10.1257/aer.101.3.238.
[55] Mai T, Mowers M, Eurek K. Competitiveness Metrics for Electricity System Technologiesno. February; 2021. p. 1–68. https://www.nrel.gov/docs/fy21osti/72549.pdf.